

Competing Acyl Transfer and Intramolecular O → N Acyl Group Migration from an Isolable O-Acylisourea

By Anthony F. Hegarty,*† Margaret T. McCormack, and Kieran Brady, Chemistry Department, University College, Cork, Ireland

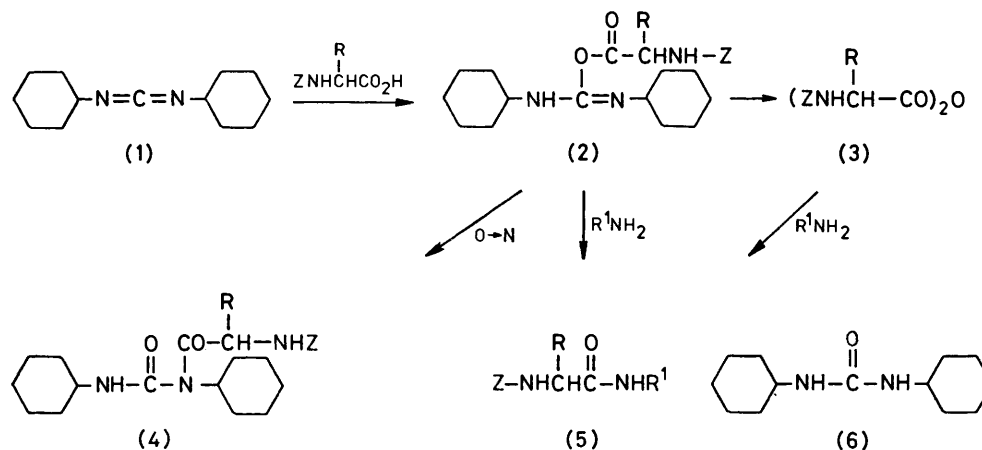
George Ferguson and Paul J. Roberts, Chemistry Department, University of Guelph, Ontario, Canada N1G 2W1

The *O*-acylisourea (16a), which is a model for the proposed intermediate in carbodi-imide condensations, and is formed on reaction of the chloride (15) with benzoate ion, was shown using *X*-ray crystallography to have the *Z*-configuration. Crystals are monoclinic, space group $P2_1/c$ with four molecules in a cell of dimensions $a = 15.732(3)$, $b = 16.246(5)$, $c = 7.628(1)$ Å, $\beta = 108.94(1)^\circ$. The structure was solved by direct methods and refined by full-matrix least-squares calculations to an R value of 0.044 for 1 281 observed reflexions. The benzoyl group is *trans* to the lone pair of the imine nitrogen and the C=N bond length is 1.286(6) Å. The isourea undergoes uncatalysed (at 25° in 1 : 4 dioxan–water, $\mu = 1.0$) O → N acyl transfer to give the *N*-acylamide (17) at pH > 7; the slow step is a *Z* → *E* isomerisation. At lower pH (3–6), *Z* → *E* isomerisation of the isourea (and thus O → N acyl transfer) is acid catalysed, but at pH < than the pK_a of (16a), intramolecular acyl transfer is inhibited by protonation of the substrate. Competing intermolecular reaction of (16a) with the solvent [to give the urea (18)] occurs at all pH. In acid, reaction is between the protonated (16a) and water and in base between the free isourea (16a) and hydroxide ion. The *O*-acylisourea also undergoes rapid intermolecular acyl transfer to a variety of amines, although reaction between the free amine and protonated isourea was too slow to be observed. The implications of these results for the design of conditions to optimise inter- (rather than intra-) molecular reactions in carbodi-imide-mediated condensations are discussed.

DICYCLOHEXYLCARBODI-IMIDE (DCC), first described by Sheehan and Hess,¹ remains the most widely used reagent in peptide syntheses and other coupling reactions (Scheme 1).² Even when other active esters are used these are usually prepared using DCC (1) and *N*-protected amino acids. The potential of solid phase peptide synthesis, introduced by Merrifield, has stimulated

these problems including the use of solvents such as DMF⁴ and additives such as *N*-hydroxysuccinimide⁵ (6a) or *N*-hydroxybenzotriazole (7).⁶ This also dictates that peptide synthesis preferentially takes place starting with the amino rather than the carboxy terminal.

Although only limited mechanistic data are available on DCC it is clear from the work of Khorana,⁷ DeTar,⁸



SCHEME 1

further interest in, and use of, this reagent.³ Reaction times are generally short and, most conveniently, both carboxylic acid and amino components can be present when the reagent is added.

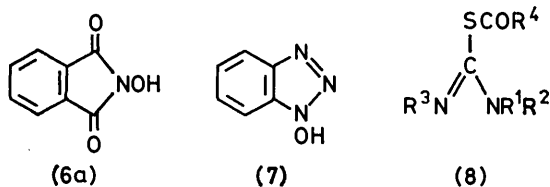
In spite of this, DCC has several disadvantages including the possibility of racemisation and the formation of unreactive *N*-acylurea adducts (4). Several methods have been used which at least partly overcome

† Present address: Chemistry Department, University College, Belfield, Dublin 4, Ireland.

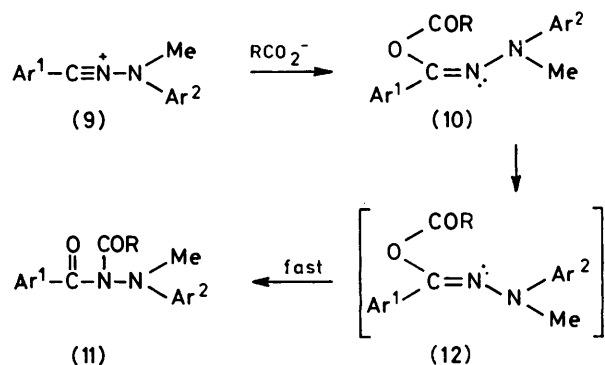
and others⁹ that several acylating species [such as (2) and (3)] are involved and the general Scheme 1 has been proposed. A limitation in studying the factors which favour competing racemisation and O → N acyl group migration in the key acylating species (2) is the fact that these adducts have not been isolated (although there is a recent report for their detection in solution).¹⁰ This is consistent with the high reactivity shown by *S*-acylthioureas (8);¹¹ in the absence of added nucleophiles, (8) undergoes rapid S → N acyl group migration and it is

expected that the oxygen analogues would react at a still faster rate. It is clear however that a rational approach to the problems inherent in the use of DCC-type reagents could be greatly enhanced if model *O*-acylisoureas were available directly for study.

We have recently shown¹² that relatively stable *O*-acylisoamides of type (10) can be synthesised by reaction of nitrilium ions (9) with carboxylates. These *O*-acyl materials (10) do undergo $O \rightarrow N$ acyl group migration



to (11) and it was shown¹² that this was limited by the rate of inversion of the imine nitrogen [(10) \rightarrow (12)]. Slowing of nitrogen inversion is therefore the key factor which permits the isolation of the *O*-acylated isoamide. We were therefore interested to discover whether *O*-acylisoureas, analogues of the proposed carbodi-imide adducts, could be isolated by a similar route. This report¹³ describes the isolation of such *O*-acylisoureas,

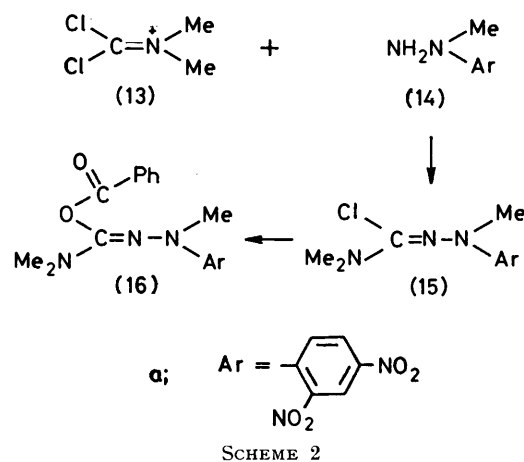


their stability in solution, and the competing reactions of intramolecular acyl transfer to the adjacent nitrogen and intermolecular transfer of the acyl group to the solvent and other nucleophiles.

RESULTS AND DISCUSSION

Formation and Crystal Structure of the Isoarea (16a).—The *O*-acylisourea (16a) was prepared according to Scheme 2. Dichloromethylenedimethylammonium chloride¹⁴ (13) was treated with *N*-methyl-*N*-(2,4-dinitrophenyl)hydrazine to give the reactive chloroformamidine (15); this on reaction with excess of silver benzoate in chloroform gave the isoarea (16a) in near quantitative yield. Attempts to prepare the corresponding chloroformamidines (15) with Ar = Ph or *p*-NO₂C₆H₄ led to cyclic products [presumably formed on reaction of the nitrilium ion from (15) with the neighbouring aromatic group].¹⁴

The crystal structure of (16a) contains discrete molecules (Figure 1) separated by normal van der Waals



distances. The molecular dimensions (Table 1) establish that N(4)–C(8) is a double bond [1.286(6) Å] comparable with the C=N bonds in acetone semicarbazone¹⁵ (1.278 Å) and in acetone 4-nitrophenylhydrazone¹⁶ (1.304 Å). The double bond geometry is clearly that with the benzoyl group *trans* to the lone pair on N(4) and the atoms bonded to N(4) and C(8) are close to coplanar [torsion

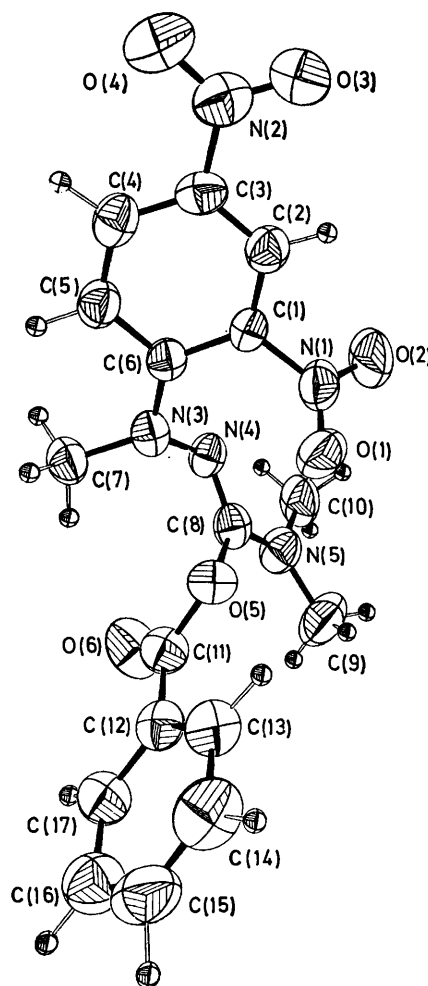


FIGURE 1 View of the molecule giving the crystallographic numbering scheme

angles N(3)–N(4)–C(8)–N(5) 179.1°, N(3)–N(4)–C(8)–C(5) –5.2°. The N(3)–N(4) bond length [1.422(6) Å] corresponds to a single bond (*cf.* 1.385 and 1.424 for the corresponding bonds in acetone semicarbazone and 4-nitrophenylhydrazone). Other molecular dimensions (Table 2) are in accord with expected values.

As can be seen from Figure 1, the conformation adopted by the molecule in the solid state is largely determined by intramolecular overcrowding effects. Thus, the planes of the nitro group N(1), O(4), O(2) and of the N(3), N(4), C(7) moiety are rotated 54.1 and 19.0° out of the plane of aromatic ring C(1)–C(6) to relieve

TABLE 1

Bond lengths (Å) with standard deviations in parentheses

C(1)C(2)	1.363(8)	C(11)C(12)	1.472(7)
C(1)C(6)	1.421(7)	C(11)O(5)	1.384(6)
C(1)N(1)	1.479(7)	C(11)O(6)	1.196(8)
C(2)C(3)	1.373(8)	C(12)C(13)	1.380(9)
C(3)C(4)	1.380(8)	C(12)C(17)	1.397(7)
C(3)N(2)	1.457(8)	C(13)C(14)	1.383(8)
C(4)C(5)	1.381(9)	C(14)C(15)	1.373(10)
C(5)C(6)	1.416(8)	C(15)C(16)	1.378(11)
C(6)N(3)	1.366(7)	C(16)C(17)	1.383(9)
C(7)N(3)	1.456(6)		
C(8)N(4)	1.286(6)	N(1)O(1)	1.213(7)
C(8)N(5)	1.334(7)	N(1)O(2)	1.216(6)
C(8)O(5)	1.383(6)	N(2)O(3)	1.225(9)
C(9)N(5)	1.435(7)	N(2)O(4)	1.214(8)
C(10)N(5)	1.452(7)	N(3)N(4)	1.422(6)

Valency angles (°) with standard deviations in parentheses

C(2)C(1)C(6)	122.7(5)	C(12)C(13)C(14)	118.7(5)
C(2)C(1)N(1)	114.9(5)	C(13)C(14)C(15)	120.3(7)
C(6)C(1)N(1)	122.0(5)	C(14)C(15)C(16)	120.8(6)
C(1)C(2)C(3)	118.9(5)	C(15)C(16)C(17)	120.1(5)
C(2)C(3)C(4)	121.3(5)	C(12)C(17)C(16)	118.5(6)
C(2)C(3)N(2)	118.4(6)		
C(4)C(3)N(2)	120.3(6)	C(1)N(1)O(1)	117.6(5)
C(3)C(4)C(5)	120.1(5)	C(1)N(1)O(2)	117.1(4)
C(4)C(5)C(6)	120.7(5)	O(1)N(1)O(2)	125.1(5)
C(1)C(6)C(5)	116.2(5)	C(3)N(2)O(3)	118.3(6)
C(1)C(6)N(3)	122.5(5)	C(3)N(2)O(4)	118.8(6)
C(5)C(6)N(3)	121.3(5)	O(3)N(2)O(4)	122.9(6)
N(4)C(8)N(5)	121.8(4)	C(6)N(3)C(7)	121.2(4)
N(4)C(8)O(5)	122.2(5)	C(6)N(3)N(4)	115.2(4)
N(5)C(8)O(5)	115.9(4)	C(7)N(3)N(4)	116.3(4)
C(12)C(11)O(5)	111.7(5)	C(8)N(4)N(3)	114.9(4)
C(12)C(11)O(6)	127.2(5)	C(8)N(5)C(9)	122.8(5)
O(5)C(11)O(6)	121.2(5)	C(8)N(5)C(10)	119.3(4)
C(11)C(12)C(13)	122.2(4)	C(9)N(5)C(10)	116.6(4)
C(11)C(12)C(17)	116.3(5)		
C(13)C(12)C(17)	121.5(5)	C(8)O(5)C(11)	118.2(5)

overcrowding between O(1) and N(4); the terminal nitro group N(2), O(3), O(4) is only rotated 3.5° out of the aromatic plane.

The geometry at N(3) is deformed slightly from trigonal planar [N(3) is 0.22 Å above the plane of C(6), C(7), N(4)]; this also helps to relieve intramolecular overcrowding between N(4) and nitro group N(1), O(1), O(2) and between the methyl C(7) and the benzoyl oxygen O(6). At the remaining nitrogen atom, N(5), there are no severe intramolecular overcrowding effects and the N(5), C(8), C(9), C(10) moiety is close to planar [N(5) 0.093 Å from the plane of C(8), C(9), C(10)].

Hydrolysis of the Isourea (16a) in Acid.—The rates of reaction of (16a) were studied spectrophotometrically in 1 : 4 dioxan–water at 25° (μ 1, KCl) over the pH range 1.0–6.0; the results are summarised in Table 3. A

TABLE 2

Final fractional co-ordinates ($\times 10^3$ for hydrogen atoms, 10^4 for others) and isotropic temperature factors (10^{-2} U/Å²) for the hydrogen atoms

	<i>x/a</i>	<i>y/b</i>	<i>z/c</i>	<i>U</i>
C(1)	5 161(3)	3 656(3)	3 337(7)	
C(2)	4 291(4)	3 601(3)	3 302(7)	
C(3)	3 925(3)	2 836(4)	3 330(7)	
C(4)	4 418(4)	2 128(3)	3 381(7)	
C(5)	5 292(4)	2 179(3)	3 372(8)	
C(6)	5 695(3)	2 953(3)	3 314(7)	
C(7)	7 075(3)	2 280(3)	3 193(7)	
C(8)	7 420(3)	4 133(3)	3 210(7)	
C(9)	8 298(4)	5 392(3)	3 609(9)	
C(10)	7 170(4)	5 052(3)	618(8)	
C(11)	8 788(4)	3 657(3)	5 369(8)	
C(12)	9 303(3)	3 674(3)	7 362(7)	
C(13)	8 970(3)	4 030(3)	8 647(8)	
C(14)	9 498(5)	4 028(4)	10 492(9)	
C(15)	10 340(5)	3 683(4)	11 024(9)	
C(16)	10 671(4)	3 328(4)	9 738(11)	
C(17)	10 161(4)	3 325(3)	7 882(8)	
N(1)	5 547(4)	4 495(3)	3 652(8)	
N(2)	3 012(4)	2 786(4)	3 401(7)	
N(3)	6 550(3)	3 012(2)	3 243(6)	
N(4)	6 721(3)	3 717(2)	2 303(5)	
N(5)	7 673(3)	4 803(3)	2 497(6)	
O(1)	5 140(3)	5 039(3)	2 633(9)	
O(2)	6 210(3)	4 596(2)	5 004(6)	
O(3)	2 705(3)	2 104(4)	3 533(8)	
O(4)	2 591(3)	3 418(3)	3 337(7)	
O(5)	7 922(2)	3 947(2)	5 020(5)	
O(6)	9 045(3)	3 429(2)	4 136(6)	
H(2)	396(2)	411(2)	335(4)	5(1)
H(4)	420(2)	156(2)	344(5)	6(1)
H(5)	567(2)	166(2)	352(5)	8(1)
H(7A)	672(2)	190(2)	216(5)	7(1)
H(7B)	720(2)	194(2)	425(4)	5(1)
H(7C)	771(2)	245(3)	332(5)	8(1)
H(9A)	888(3)	522(3)	371(6)	13(2)
H(9B)	818(3)	594(3)	298(7)	14(2)
H(9C)	821(3)	551(3)	489(8)	15(2)
H(10A)	691(3)	457(3)	–19(6)	10(1)
H(10B)	667(3)	542(3)	65(6)	10(1)
H(10C)	758(3)	535(3)	8(7)	13(2)
H(13)	837(2)	435(2)	825(5)	8(1)
H(14)	929(2)	433(2)	1 134(5)	10(1)
H(15)	1 080(2)	378(2)	1 229(6)	11(1)
H(16)	1 132(2)	305(2)	1 011(5)	10(1)
H(17)	1 043(3)	306(2)	969(6)	10(1)

TABLE 3

Observed first-order rate constants for the hydrolysis of the isourea (16a)^a

pH	$10^4 k_{\text{obs}}/$ s^{-1}	% Urea (18)	$10^4 k_{\text{inter}}/$ s^{-1}	$10^4 k_{\text{intra}}/$ s^{-1}
1.00	1 400	93	1 302	98
1.20	1 370	92	1 260	109
1.50	1 340	88	1 179	161
1.80	1 400	83	1 160	238
2.00	1 340	80	1 070	268
2.05	1 300	78	1 010	286
2.15	1 180	75	890	295
2.20	1 200	73	876	324
2.30	1 130	70	970	339
2.40	755	66	498	257
2.50	720	65	468	252
2.65	590	60	355	236
2.80	455	55	251	205
3.00	454	50	227	227
3.50	232	41	95	137
4.00	76	37	26	48
4.50	26	35	9.8	17
5.00	9.2	33	3.1	6.1
6.00	1.0	33	0.32	0.68

^a In the pH region 1–6 in 1 : 4 dioxan–water at 25° in the absence of added buffer species.

plot of $\log k_{\text{obs}}$ against pH (Figure 2) shows clearly that the reaction rate is proportional to acid concentration at $\text{pH} > 3.5$ but becomes pH independent at low pH. Because of the complexity of the pH-rate profile, the acid, neutral, and basic regions will be considered separately.

(i) *Reaction at pH 0–6.* Although the overall reaction

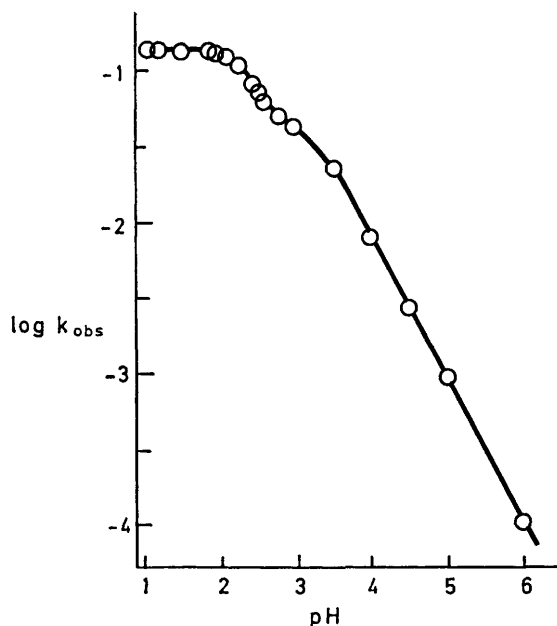
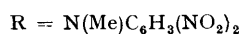
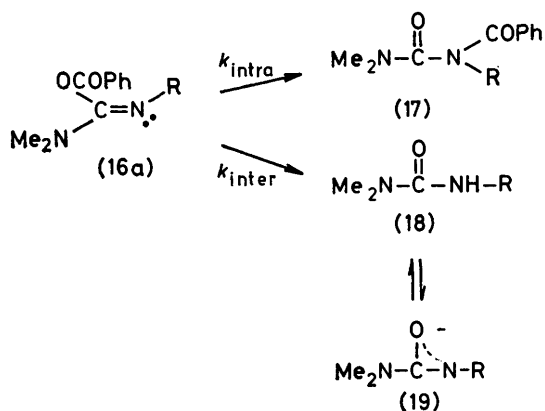


FIGURE 2 Plot of $\log(k_{\text{obs}}/\text{s}^{-1})$ for the reaction of the isourea (16a) in 4:1 water-dioxan at 25° (μ 1.0). The line is theoretical, being derived from a combination of equations (1) and (2), with the values of the constants given in the text

shows acid catalysis in this region, the changeover of the rate to pH independence at low pH does not occur in a simple fashion (as in a regular titration curve); instead there are clearly two 'breaks' in the curve at pH ca. 3.0 and 2.0.

Two products, the *N*-acylurea (17) (arising from an intramolecular $\text{O} \rightarrow \text{N}$ acyl transfer) and the urea (18)



[deacylation of (16a)] are formed in varying amounts over this pH region. This was shown by t.l.c. analysis (see Experimental section) and by the actual separation

and isolation of both (17) and (18) using preparative t.l.c. Since the u.v. spectra of (17) and (18) are similar in acidic or neutral solution (with absorption maxima at 350 and 340 nm, respectively), analysis of the relative amounts of (17) and (18) was achieved by basification of the solution (to pH ca. 14) following reaction of (16a) at low pH. Since the urea (18) was converted into its conjugate base (19) at high pH whereas (17) remained unchanged, the concentration of the anion could be determined at 490 nm and that of the *N*-acylurea (17) at 350 nm. Preliminary experiments showed that (17) is not deacylated to (18) in acid solution and that although

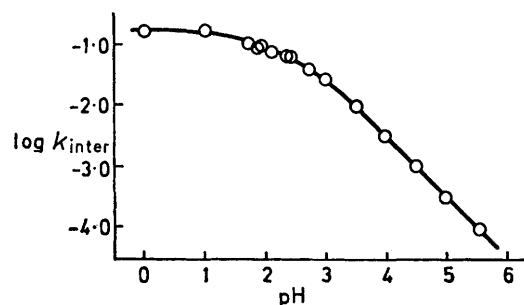


FIGURE 3 The log dependence of the rate constants (in s^{-1}) for the formation of the amide (18) from the isourea (16a) (25° ; 4:1 water-dioxan). The line describes a simple titration curve [see equation (1)]

deacylation of (17) does occur in base, the rate of conversion is slow enough to permit accurate and reproducible measurements. The results obtained [expressed as % urea (18) formed] are also summarised in Table 3.

Since (17) and (18) are formed by parallel (rather than consecutive) reactions, it is possible using the product analysis data to calculate k_{intra} and k_{inter} , the observed

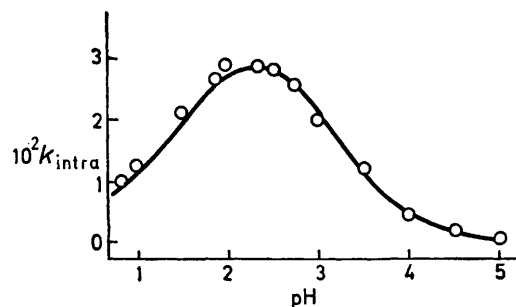


FIGURE 4 The bell-shaped dependence of k_{intra} [formation of the *N*-acylurea (17)] (in s^{-1}) measured at 25° in 4:1 water-dioxan. The line is theoretical [see equation (2)] and the values of the constants used are given in the text

rate constants for the formation of (17) and (18), respectively. These are shown as plots in Figures 3 and 4.

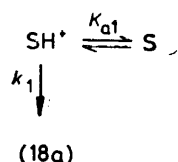
Intermolecular reaction. Intermolecular hydrolysis of (16) to (18) presents the simplest pH-rate profile, being in the form of a titration curve (Figure 3). This is consistent with equation (1), derived from Scheme 3, where S and SH^+ are the isourea (16a) and the protonated isourea respectively; the values of k_1 and $\text{p}K_{a1}$ which best fit this curve are 0.15 s^{-1} and 2.36, respectively.

This implies that the isourea (16a) is protonated at low pH. This was confirmed by the appearance of a new absorption at 280 nm. An approximate pK_{a1} value (of 2.0 ± 0.2) for (16a) was estimated spectrophotometrically. Because of the high reactivity of (16a) at

$$k_{inter} = k_1 K_{a1} / (K_{a1} + a_{H^+}) \quad (1)$$

low pH (see Figure 2) the stopped-flow spectrophotometer was used to estimate the optical density of (16a) at various pH values by extrapolation back to 0% reaction. Thus we conclude that intermolecular hydrolysis of (16a) occurs at pH < 6 only *via* reaction of water with the protonated isourea.

Intramolecular isomerisation. The competing parallel reaction, intramolecular isomerisation to (17), shows a more complex pH dependency (Figure 4). At pH 3–6, the rate is proportional to acid concentration (as is the



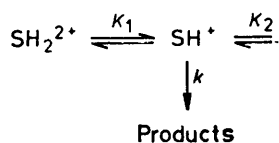
SCHEME 3

intermolecular reaction), but the fraction of isomerisation that occurs is greater at all pH values in this region (k_{intra}/k_{inter} reaches a constant value of *ca.* 2.0). At low pH however the formation of (17) is inhibited by acid so that intermolecular hydrolysis becomes the dominant reaction. The pH-rate profile for intramolecular acylation (Figure 4) is closely fitted by the equation (2) for a bell-shaped curve, often observed in enzyme catalysed

$$k_{intra} = k a_{H^+} K_1 / (a_{H^+}^2 + a_{H^+} K_1 + K_1 K_2) \quad (2)$$

reactions, with $k = 6 \times 10^{-2} \text{ s}^{-1}$, $K_1 = 1.25 \times 10^{-2}$, and $K_2 = 2.5 \times 10^{-3}$.

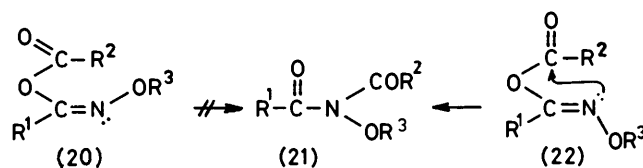
Such bell-shaped curves normally arise through the operation of a Scheme such as 4. In this only the



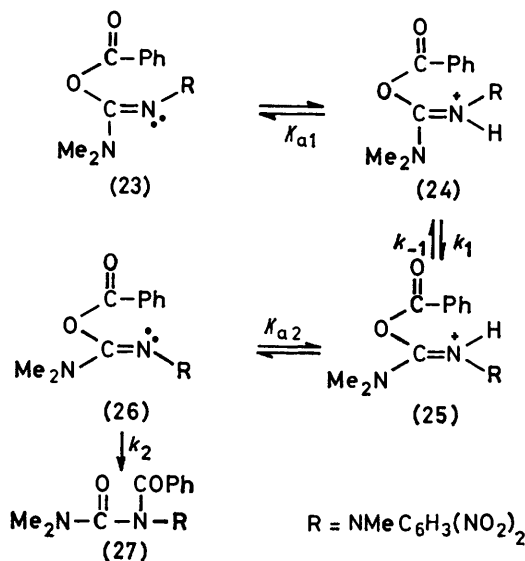
SCHEME 4

monoprotonated form of the substrate (SH^+) undergoes reaction, SH_2^{2+} and S being unreactive. Scheme 4 implies that at pH < 2 the major form of the substrate present was diprotonated, the monoprotonated species being dominant at pH 2–4. However, we have observed spectral evidence for only one protonation-deprotonation equilibrium (with a pK_a of 2.0) in the pH region 0–6; moreover if the substrate was successively mono- and di-protonated as the acidity of the solution is increased (at pH *ca.* 4 and 2 respectively) then this would be apparent from the observed intermolecular rate constants (making the reasonable assumption that the

diprotonated substrate would react more rapidly with water than the monoprotonated form). Other possible mechanisms (such as the acid dependent partitioning of a tetrahedral intermediate), which might give rise to the observed pH independence of k_{intra} , can also be ruled out.



As the crystal structure of (16a) has shown, the acyl group and lone pair on the adjacent nitrogen are *trans*. We have recently shown¹⁷ using isolable *Z*- and *E*-isomers (20) and (22) that only the *E*-isomer (22) rearranges to the imide form (21). Thus *Z* → *E* isomerisation of (16a) must occur prior to acyl group transfer to nitrogen. The possibility therefore arises that the acid catalysis acts on the *Z* → *E* isomerisation step, rather than on the intramolecular acyl transfer step itself. Scheme 5 illustrates this possibility; in Scheme 5 it is assumed that the formation of (27) occurs only from the *E*-isomer (26) and that isomerisation about the C=N bond is acid catalysed [*via*, say (24)]. If the *Z* → *E* isomerisation step described by k_1 is rate determining [with (25) and (26) in low steady state concentration] then Scheme 5



SCHEME 5

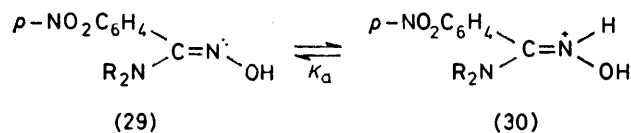
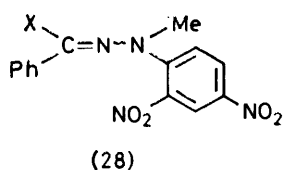
gives a rate expression similar to that observed [equation (2)] with $kK_1 = k_1 k_2 K_{a2} / k_{-1}$, $K_1 = K_{a1} + k_2 K_{a2} / k_{-1}$, and $K_1 K_2 = k_2 K_{a1} K_{a2} / k_{-1}$.

From the fit to the observed values listed above, two values (3.2×10^{-3} and 2.0×10^{-2}) are estimated from the quadratic equation for K_{a1} . The value of 3.2×10^{-3} is chosen as the correct one since this is closest to the observed K_{a1} value obtained in the intermolecular reaction (4.4×10^{-3}). The other values for the constants arising from this are $k_1 = 7.9 \times 10^{-2}$ and $k_2 K_{a2} / k_{-1} =$

9.7×10^3 ; the second acidity constant K_{a2} cannot be obtained directly from this expression.

Scheme 5 assumes that $Z \rightarrow E$ isomerisation between the neutral forms (23) and (26) is slow. This is reasonable when compared to the rate constants measured for uncatalysed isomerisation of the corresponding *O*-acylhydrazides (28; X = CH₃CO₂), k $6.3 \times 10^{-5} \text{ s}^{-1}$, and *O*-methylhydrazides (28; X = MeO), k $1.8 \times 10^{-4} \text{ s}^{-1}$, at 70° in chlorobenzene.¹² Although acid catalysis of isomerisation of (28; X = CH₃CO₂ or MeO) could not be observed (intermolecular hydrolysis being in all cases faster), the corresponding amidoxime system (29) shows very marked acidic catalysis with $Z \rightarrow E$ isomerisation rate for (30) being 10^5 greater than from (29).¹⁸ The acidity of (29) (K_a 4×10^{-4}) and the rate of $Z \rightarrow E$ isomerisation of (30) [6.8 s^{-1} when R₂ is (CH₂)₂O(CH₂)₂], which are measured directly, are in the same range as those estimated for (24) adding support to the proposed mechanism in Scheme 5.

Although we have labelled the protonation site of the *O*-acylisourea (16a) as the imine nitrogen (24), the



possibility also arises that the dimethylamino group of this amidine-type system could be the basic site. We believe that this is unlikely for two reasons: (a) the isourea (16a) shows a large spectral change on protonation (loss of the absorption at 280 nm); (b) it is difficult to see how protonation of the NMe₂ group would lead to such a profound rate difference; substituent effects at this site are usually small for the corresponding imine systems.¹⁹ In fact protonation on the Me₂N group would be expected to increase (rather than decrease) the double bond character of the imine group.

There is therefore a subtle balance between the inter- and intra-molecular reactions of the *O*-acylisourea. A key finding of this work is that moderate amounts of acid increase both intermolecular reactions and $Z \rightarrow E$ isomerisation (which is a necessary precondition for intramolecular acyl group migration) to the same extent. Intermolecular reaction can however be favoured in more highly acidic solution (where $a_{\text{H}^+} \gg K_{a1}$). Since this is the desired reaction in carbodi-imide mediated condensations (Scheme 1), it would appear that optimum conditions would involve acidic solution. In the case of the isourea model (16a) which we have used, intermolecular reaction tends to be the sole reaction only at $\text{pH} < 2$; however with other more basic isoureas such

as (2), whose $\text{p}K_a$ values are > 6 , intermolecular reaction can be enhanced in more moderately acidic solution.

(ii) *Hydrolysis of the isourea at pH > 6*. The observed rate constants for the hydrolysis of the isourea (16a) in basic solution are listed in Table 4. Again two products

TABLE 4

Observed rate constants for reaction of the isourea (16a) ^a							
pH	7.0	8.00	8.64	9.47	10.21	10.97	
$10^5 k_{\text{obs}}/ \text{s}^{-1}$	1.6	1.5	1.41	2.24	5.62	18.6	
$10^5 k_{\text{inter}}/ \text{s}^{-1}$	0.80	0.71	0.77	1.65	5.15	18.2	
pH	11.44	11.70	12.03	12.50	12.80	13.03	13.21
$10^5 k_{\text{obs}}/ \text{s}^{-1}$	55	100	224	708	1 480	2 510	3 980
$10^5 k_{\text{inter}}/ \text{s}^{-1}$	55	100	224	708	1 480	2 510	3 980

^a Measured in 4 : 1 water-dioxan (μ 1.0) at 25°.

were observed, the *N*-acylamide (17) and the amide (18), and the relative amounts of these were determined spectrophotometrically as described above, and the derived k_{inter} values [formation of (18)] are included in Table 4. From the plot of $\log k_{\text{inter}}$ and $\log k_{\text{intra}}$ against pH shown in Figure 5, it is seen that both the intermolecular hydrolysis and the intramolecular isomerisation to (17) become pH independent at $\text{pH} > 7$, while base catalysed hydrolysis of (16a) becomes important at $\text{pH} > 9$.

These results are best explained in terms of the mechanistic Scheme 6, where k_3 ($= 7.5 \times 10^{-6} \text{ s}^{-1}$) is the rate of uncatalysed $Z \rightarrow E$ isomerisation of the isoimide and k_4 ($= 0.25 \text{ l mol}^{-1} \text{ s}^{-1}$) and k_5 ($= 7.0 \times 10^{-6} \text{ s}^{-1}$) are the

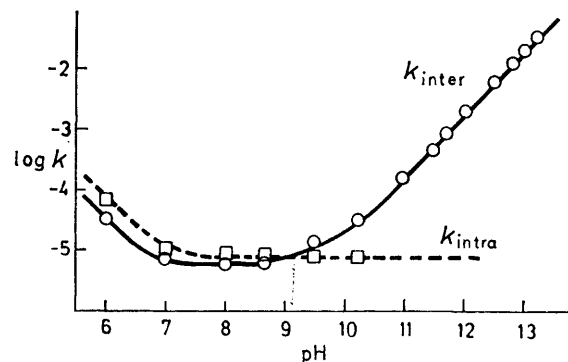


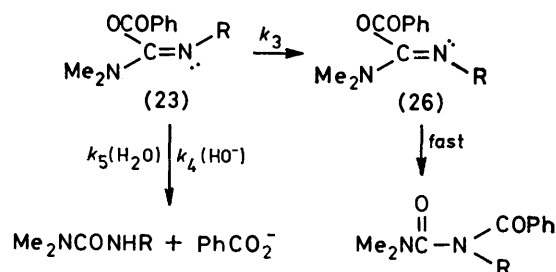
FIGURE 5 Plots of $\log k_{\text{inter}}$ and $\log k_{\text{intra}}$ for the competing reactions of the isourea (16a) at $\text{pH} > 6$. At high pH (broken line) it is assumed that k_{intra} remains pH independent, although the quantity of *N*-acylisourea formed was too small to be measured with accuracy.¹⁹

rate constants for hydroxide catalysed and pH independent hydrolysis of the isoimide respectively.

The rates of uncatalysed imine isomerisation have been intensively studied;^{19,20} however the rate constants for isomerisation cover a very large range, so that it is difficult to determine whether the k_3 value we have observed is reasonable for such a process. The key factor appears to be the nature of the substituent (R) attached to nitrogen. It is clear however from the similarity in $\text{p}K_a$ of (16a) and the amidoxime (29) that the OH and

$N(\text{Me})\text{C}_6\text{H}_3(\text{NO}_2)_2$ groups have about the same electron-withdrawing power, and uncatalysed $Z \rightarrow E$ isomerisation of the amidoxime [29; $\text{R}_2 = (\text{CH}_2)_2\text{O}(\text{CH}_2)_2$] has a rate constant ($1.3 \times 10^{-4} \text{ s}^{-1}$, measured at 57° in water) in the same range which we have reported for k_3 .

Intermolecular reaction of hydroxide ion with the isourea (23) could occur at either the carbon-oxygen or carbon-nitrogen double bonds, in both cases leading to the observed products. Although it is difficult to distinguish between these two possibilities (in the



SCHEME 6

absence of labelling studies), we favour reaction at the acyl carbon * since this is the mode of reaction shown to occur in basic solution with cyclic *O*-acylisoamides, and amine nucleophiles (see below) also react at this site.

Reaction of the Isourea with Amines.—We have also determined the rates of aminolysis of the isourea (16a) with secondary amines. Reaction occurs only between the free amine and the unprotonated isourea; Figure 6 shows a plot of $\log k_N$ against pH for the amine morpholine. It is clear that at high pH the rate of reaction was pH independent while at pH less than the $\text{p}K_a$ of the amine, the observed rate of reaction with the amine, k_{NT} ,

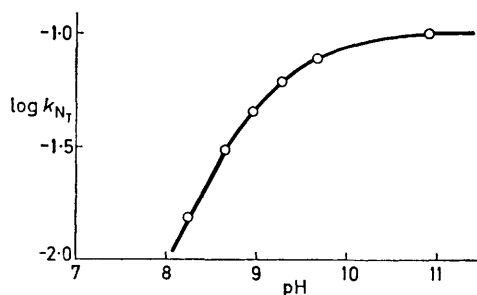


FIGURE 6 Plot of the log of the second-order rate constants, k_{NT} , for the reaction of morpholine with the isourea (16a) (at 25° ; in 4:1 water-dioxan). The k_{NT} values refer to total buffer concentration and are corrected for the (minor) reaction with the solvent

was proportional to the concentration of unprotonated amine present. It is conceivable that reaction would also occur between morpholine and the protonated substrate (24). However in acidic solution ($\text{pH} < 6$) no

* However at the highest pH values studied ($\text{pH} 12\text{--}13$) the maximum amount of urea formed reached a constant value of 90–92%. This may have been due to competing base catalysed $\text{O} \rightarrow \text{N}$ isomerisation of the *O*-acylisourea (although this is unlikely since further hydrolysis of the *N*-acylurea would have been observed at high pH); a more plausible explanation is competing attack by hydroxide ion at the $\text{C}=\text{N}$ bond.

amine catalysis was observed. Apparently the $\text{p}K_a$ values of the substrate and the amine are so far apart (>6 units) that the concentrations of the reactive species (protonated substrate and free amine) are too small for aminolysis to compete with hydrolysis in acidic solution. This is almost certainly not true with simple *O*-acyl-isoureas such as (2) whose $\text{p}K_a$ values are much closer to those of typical amines. The highest rate of aminolysis of the isourea will thus occur close to its $\text{p}K_a$; it is clear therefore that the optimum pH for the coupling reaction is just below the $\text{p}K_a$ for the isourea intermediate. Intermolecular aminolysis will still be rapid under these conditions while intramolecular rearrangement will be suppressed.

The rates of reaction of a number of selected amines (previously found to give well behaved Brønsted plots) with the neutral isourea (16a) were measured in basic solution. In all cases the aminolysis rates were fast and proportional to free amine concentration (with no second-order dependence on amine concentration, even at the highest amine concentrations used). The derived second-order rate constants are summarised in the Brønsted plot of Figure 7. The observed slope (or β

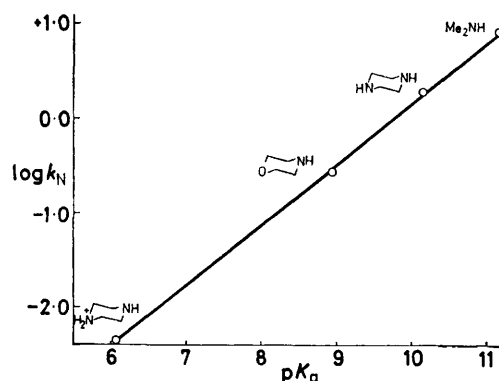


FIGURE 7 Brønsted plot of the log of the second-order rate constants ($\text{l mol}^{-1} \text{ s}^{-1}$) for the reaction of (free) secondary amines with the isourea (16a) in water-dioxan (4:1) at 25°

value) of $+0.66$ is within the range observed for other ester aminolyses and can be used to calculate the rates of reaction of the isourea with other amine bases.

In conclusion, the isourea (16a) which was shown to have the *Z*-configuration undergoes competing inter- and intra-molecular reactions. Intramolecular isomerisation to the *N*-acyl form is limited by substrate $Z \rightarrow E$ isomerisation which is catalysed ($\text{pH} 2\text{--}6$) or inhibited ($\text{pH} < 2$) by acid or may occur (at high pH) by a slow uncatalysed process. Intermolecular reaction with water only becomes dominant at $\text{pH} (< 2)$ less than the $\text{p}K_a$ of the substrate, while reaction with hydroxide ion is much faster than any of the competing reactions at high pH. Finally, although amines react rapidly with the isourea (16a) in basic solution, the rate of reaction with the protonated substrate is slower than reaction with the solvent (although this may not be true with other, more basic, *O*-acylisoureas). The optimum conditions which favour intermolecular reaction with nucleophiles (such as

amines), rather than competing intramolecular isomerisation, are therefore either (a) at a pH 1–2 units less than the pK_a of the isourea or (b) at high pH, close to the pK_a of the amine.

EXPERIMENTAL

N'-[Chloro(dimethylamino)methylene]-*N*-2,4-dinitrophenyl-*N*-methylhydrazine (15a).—*N*-Methyl-2,4-dinitrophenylhydrazine (1.8 g), prepared from 1-chloro-2,4-dinitrobenzene and *N*-methylhydrazine in ethanol, was dissolved in dry chlorobenzene (70 ml) under nitrogen and refluxed. Solid dichloromethylenedimethylammonium chloride (1.30 g) was added over 10 min, the apparatus being maintained under nitrogen. Evolution of HCl occurred, and the solution became homogeneous and deep red. The mixture was refluxed for a further 30 min when t.l.c. [R_F 0.41 on silica gel using 3 : 2 ethyl acetate–light petroleum b.p. (40–60°) as eluant] indicated complete reaction. Evaporation of the solution gave the hydrazine (15a) (88%), m.p. 102°, on recrystallisation from benzene–hexane, δ 3.10 (6 H, NMe₂) and 3.22 (3 H, NMe) (Found: C, 39.7; H, 4.2; Cl, 11.3; N, 23.5. C₁₀H₁₂ClN₅O₄ requires C, 39.8; H, 4.0; Cl, 11.7; N, 23.2%).

O-Benzoyl-*NN*-dimethyl-*N'*-(*N*-methyl-2,4-dinitroanilino)-isourea (16a).—Excess of solid silver benzoate (1.0 g) was added to a solution of (15a) (0.20 g) in dry chloroform (50 ml) at reflux. The mixture was refluxed for 10–12 min until t.l.c. [R_F of product was 0.30 on silica gel using 3 : 2 ethyl acetate–light petroleum (b.p. 40–60°) as eluant]. On removal of silver salts, the isourea (16a) was obtained on evaporation on the chloroform and had m.p. 124–125° (90%; from chloroform–pentane), ν_{\max} . 1 750 (C=O) cm⁻¹; δ 3.08 (9 H, NMe₂, NMe); on scale expansion this gave δ 3.10 (6 H, NMe₂) and 3.05 (3 H, NMe) (Found: C, 52.4; H, 4.4; N, 18.3. C₁₇H₁₇N₅O₆ requires C, 52.7; H, 4.4; N, 18.1%).

An attempt was made to prepare the *O*-acetyl analogue as follows. Silver acetate (1.0 g) was added to a solution of the chloride (15a) in chloroform (40 ml) [dried by passing down an alumina (W200, basic, activity 1) column]. The solution was refluxed for 30 min when t.l.c. indicated two products including *NN*-dimethyl-*N'*-(*N*-methyl-2,4-dinitroanilino)urea [R_F 0.28 on silica gel, using 3 : 2 ethyl acetate–light petroleum (b.p. 40–60°) as eluant]. The solution was filtered free of silver salts and concentrated to 5 ml; addition of diethyl ether precipitated a solid, m.p. 116–117° (68%); (from chloroform–ether), which was identified as ethyl *N*-(*N*-methyl-2,4-dinitroanilino)carbamate, ν_{\max} . 1 740 (C=O) and 3 370 (N–H) cm⁻¹; δ 1.23 (3 H, t, CH₃), 4.13 (2 H, q, CH₂) and 3.35 (3 H, s, NMe) (Found: C, 42.5; H, 4.3; N, 19.9. C₁₀H₁₂N₄O₆ requires C, 42.3; H, 4.2; N, 19.7%).

The carbamate was also synthesised unambiguously from equimolar quantities of *N*-methyl-*N'*-(2,4-dinitrophenyl)hydrazine, ethyl chloroformate, and triethylamine in chloroform.

N'-Benzoyl-*NN*-dimethyl-*N'*-(*N*-methyl-2,4-dinitroanilino)-urea (17).—The *O*-benzoylisourea (16a) (0.50 g) was dissolved in acetonitrile (5 ml) and added to 1 : 4-dioxan-water (v/v) solution buffered at pH 5.0. The mixture was maintained at 30° for 1 h and a yellow solid was then precipitated by the addition of ice-water. T.l.c. indicated two components, the *N*-benzoylurea (17) (R_F 0.30) and the urea (18) [R_F 0.05 using silica gel and 7 : 3 ethyl acetate–light petroleum ether (b.p. 40–60°) as eluant]. The *N*-benzoyl-

urea (17) was isolated by preparative t.l.c. using the same eluant and had m.p. 68° (Found: C, 52.7; H, 4.4; N, 18.1. C₁₇H₁₇N₅O₆ requires C, 53.0; H, 4.6; N, 18.3%).

NN-Dimethyl-*N'*-(*N*-methyl-2,4-dinitroanilino)urea (18).—The chloroformamide (15a) (0.20 g) dissolved in acetone (2 ml) was added to 1 : 1 acetone–water (100 ml) and maintained at 35° for 15 min. On cooling and the addition of ice–water the urea crystallised, m.p. 191–192° (from acetone–hexane) (Found: C, 42.6; H, 3.7; N, 25.2. C₁₀H₁₆N₅O₅ requires C, 42.7; H, 3.6; N, 25.0%).

Kinetic Method.—All rate measurements were carried out on a Perkin-Elmer model 124 or Unicam model 800B spectrophotometer, or a Cary 14B spectrophotometer (equipped with an external pH stat to maintain the pH constant in the absence of added buffer species).²¹ The instruments were equipped with multiple thermostatable cell compartments and external recorders.

The substrate was prepared as a concentrated solution (usually 10⁻²M) in acetonitrile and reaction was initiated by the addition of a drop of this substrate solution to the cell containing the equilibrated reaction solution. The rates of hydrolysis were followed by recording the change in optical density with time at a suitable wavelength (which was established by an initial repetitive scan of the u.v.–visible region). Good pseudo-first-order plots of log (O.D._∞ – O.D._{*t*}) were obtained using experimental infinity values. The pH values quoted throughout are the indicated values obtained in 1 : 4 dioxan–water using a pH electrode which had been standardised in aqueous buffers in the same pH region. Since the isourea (16a) was found to rearrange to the *N*-benzoylurea (17) in the presence of light, the stock solution of the isourea was prepared fresh each day and then protected from light.

pK_a Determination.—Since below pH 1.0 the rates of hydrolysis of (16a) were very rapid (*t*_½ < 10 s) the dissociation constant was estimated using a Durrum–Gibson model D-110 stopped-flow spectrophotometer, equipped with Kel-F components and log converter. The substrate was dissolved at pH 6.0 (where minimum reactivity is observed) in 1 : 4 dioxan–water using 1 × 10⁻³M-buffer. This was added to an equal concentration of a concentrated (0.1–1.0M) buffer in 1 : 4 dioxan–water in the pH range 0–3. The optical density at 287 nm was recorded at each pH as a function of time. Extrapolation of the oscilloscope trace back to 0% reaction gave the optical density (O.D.) of the substrate at various pH values (0.2 units apart close to the pK_a). Theoretical titration curves were plotted using equation (3) and the actual pK_a of the substrate was computed by comparison with the curve which best fitted the experimental data.

$$O.D._{obs} = O.D._{max} \frac{K_a}{(a_{H^+} + K_a)} \quad (3)$$

Product Analysis.—The relative amounts of the urea (18a) and the *N*-benzoylurea (17) formed at the end of a kinetic experiment were determined as follows. The *O*-benzoylisourea (16a) was prepared (1 × 10⁻³M) in acetonitrile and protected from light. A portion (20 μl) of this solution was added to 2.5 ml of a buffer solution (10⁻²M-buffer; 1 : 4 dioxan–water at 25°). When reaction was complete (10*t*_½, see Table 1), 10N-NaOH (0.2 ml) was added to the cell and the absorption of the anion (19) was measured at 490 nm. The absorption of the *N*-benzoylurea (17), which did not change on basification, was also determined at 340 nm as a complimentary check. Slow hydrolysis of the *N*-benzoylurea (17) to the urea (18) occurred under the highly basic

conditions used for the determination. Thus the O.D. at 490 nm slowly increased and that at 340 nm decreased with time. A correction was made for this by extrapolating the O.D. versus time plots back to the time of mixing.

Since both light-catalysed and spontaneous O \rightarrow N benzoyl group migration can also occur, (16a) was purified by recrystallisation and/or preparative t.l.c. shortly before product analysis was carried out. The results (Table 1) are reproducible with different samples of the chloride and were checked by an independent worker.

Crystal Data.— $C_{17}H_{17}N_5O_6$, $M = 387.4$. Monoclinic, $a = 15.732(3)$, $b = 16.246(5)$, $c = 7.628(1)$ Å, $\beta = 108.94(1)^\circ$, $U = 1844.0$ Å³, $Z = 4$, $D_c = 1.39$ g cm⁻³, $F(000) = 808$, Mo- K_α radiation, $\lambda = 0.71069$ Å, μ (Mo- K_α) = 0.7 cm⁻¹. Systematic absences $h0l$ if $l = 2n + 1$, $0k0$ if $k = 2n + 1$, determine space group $P2_1/c$ (C_{2h}^5 , No. 14) uniquely.

Crystallographic Measurements.—Approximate cell constants were obtained from Weissenberg and precession photography, accurate unit cell data were obtained by a least-squares fit of the values of $\pm 2\theta$ for 12 strong general reflections measured on our diffractometer. Intensities were measured on a Hilger and Watts Y-290 PDP8-1 controlled four-circle diffractometer as described previously.²² Data were corrected for Lorentz and polarisation factors but not for adsorption which is negligible. Of the 2223 reflections with $\theta \leq 22^\circ$, 1281 having intensities $> 3.0\sigma(I)$ were employed in the subsequent structure analysis and refinement.

The structure was solved by direct methods using the SHELX system of programs.²³ All hydrogen atoms were located from a difference synthesis after initial full-matrix least-squares refinement of the C, N, and O parameters. In the final round of calculation, all positional parameters were refined. The hydrogen atoms were allowed isotropic thermal parameters and the remaining atoms allowed to vibrate anisotropically. At convergence, $R = 0.044$ and $R' = \{\sum w\Delta^2/\sum wF_o^2\}^{1/2} = 0.043$. A final difference synthesis was devoid of any chemically significant features. In the least-squares calculations, the weights used were derived from the counting statistics. The scattering factors of ref. 24 were used for hydrogen atoms and those of ref. 25 for non-hydrogen atoms.

Atomic co-ordinates and their standard deviations are in Table 2. Table 1 contains details of molecular geometry. A view of the molecule with our numbering scheme is in Figure 1. A list of calculated and observed structure factors, and thermal parameters have been deposited as Supplementary Publication No. SUP 22720 (15 pp.).*

G. F. thanks the National Research Council of Canada for the award of an operating grant and M. T. McC. and K. B.

thank the Irish Government for a State Maintenance Grant for Research.

[9/1285 Received, 13th August, 1979]

* For details of Supplementary Publications see Notice to Authors No. 7 in *J.C.S. Perkin II*, 1979, Index issue.

REFERENCES

- ¹ J. C. Sheehan and G. P. Hess, *J. Amer. Chem. Soc.*, 1955, **77**, 1067; J. C. Sheehan, M. Goodinan, and G. F. Hess, *ibid.*, 1956, **78**, 1367.
- ² See, for example, M. Bodanszky, Y. S. Klausner, and M. A. Ondetti, 'Peptide Synthesis,' Wiley, New York, 1976, 2nd edn.
- ³ R. B. Merrifield, *J. Amer. Chem. Soc.*, 1963, **85**, 2149; J. M. Stewart and J. D. Young, 'Solid Phase Peptide Synthesis,' Freeman, San Francisco, 1969.
- ⁴ See, for example, D. J. Kroon and E. T. Kaiser, *J. Org. Chem.*, 1978, **43**, 2107 and references therein.
- ⁵ F. Wunsch and F. Drees, *Chem. Ber.*, 1966, **99**, 110; F. Weygand, D. Hoffmann, and E. Wunsch, *Z. Naturforsch.*, 1966, **21b**, 426; J. E. Zimmerman and G. W. Anderson, *J. Amer. Chem. Soc.*, 1964, **86**, 1839.
- ⁶ W. König and R. Geiger, *Chem. Ber.*, 1970, **103**, 788, 2034; D. G. McCarthy, A. F. Hegarty, and B. J. Hathaway, *J.C.S. Perkin II*, 1977, 224; D. G. McCarthy and A. F. Hegarty, *ibid.*, p. 231.
- ⁷ M. Smith, J. G. Moffatt, and H. G. Khorana, *J. Amer. Chem. Soc.*, 1958, **80**, 6204.
- ⁸ D. F. DeTar and R. Silverstein, *J. Amer. Chem. Soc.*, 1966, **88**, 1013, 1020; D. F. DeTar, R. Silverstein, and F. F. Roberts, *ibid.*, p. 1024.
- ⁹ J. Rebek and D. Feitler, *J. Amer. Chem. Soc.*, 1974, **96**, 1606.
- ¹⁰ A. Arendt and A. M. Kolodziefczyk, *Tetrahedron Letters*, 1978, 3367.
- ¹¹ R. F. Pratt and T. C. Bruice, *J. Amer. Chem. Soc.*, 1972, **94**, 2823.
- ¹² M. T. McCormack and A. F. Hegarty, *J.C.S. Perkin II*, 1976, 1701.
- ¹³ Some of the results have been published in preliminary form, A. F. Hegarty, M. T. McCormack, G. Ferguson, and P. J. Roberts, *J. Amer. Chem. Soc.*, 1977, **99**, 2015.
- ¹⁴ Z. Janousek and H. G. Viehe in 'Iminium Salts in Organic Chemistry,' eds. H. Böhme and H. G. Viehe, Wiley, New York, 1976, p. 343.
- ¹⁵ D. V. Naik, and G. J. Palenik, *Acta Cryst.*, 1974, **B30**, 2396.
- ¹⁶ G. Menczel, G. Samay, and K. Simon, *Acta Chim. Acad. Sci. Hung.*, 1972, **72**, 441.
- ¹⁷ D. G. McCarthy and A. F. Hegarty, *J.C.S. Perkin II*, 1977, 1080, 1085.
- ¹⁸ K. J. Dignam and A. F. Hegarty, *J.C.S. Chem. Comm.*, 1976, 863.
- ¹⁹ J. M. Lehn, *Fortschr. Chem. Forsch.*, 1970, **15**, 311.
- ²⁰ H. Kessler, *Angew. Chem. Internat. Edn.*, 1970, **9**, 219.
- ²¹ A. F. Hegarty and L. N. Frost, *J.C.S. Perkin II*, 1973, 1719.
- ²² E. C. Alyea, S. A. Dias, G. Ferguson, and R. J. Restivo, *Inorg. Chem.*, 1977, **16**, 2329.
- ²³ G. M. Sheldrick, 1976, SHELX, a program system for crystal structure determination, University of Cambridge.
- ²⁴ D. T. Cromer and J. B. Mann, *Acta Cryst.*, 1968, **A24**, 321.
- ²⁵ R. F. Stewart, E. R. Davidson, and W. T. Simpson, *J. Chem. Phys.*, 1965, **42**, 3175.